Induction of pancreatic neoplasia in the *KRAS*/*TP53* Oncopig

Pinaki Mondal[1,2], Neesha S. Patel[1,2], Katie Bailey[1,2], Audrey J. Lazenby[3], Mark A. Carlson[1,2,4]

1. Department of Surgery, University of Nebraska Medical Center, Omaha, Nebraska
2. Department of Surgery and VA Research Service, Nebraska-Western Iowa Health Care System, Omaha, NE
3. Department of Pathology, University of Nebraska Medical Center, Omaha, Nebraska
4. Department of Genetics, Cell Biology and Anatomy, University of Nebraska Medical Center, Omaha, Nebraska

Running title: Pancreatic neoplasia in the Oncopig

Financial Support: this work was funded by grants from the University of Nebraska Medical Center, the Buffett Cancer Center, and the National Cancer Institute.

Correspondence:
Mark A. Carlson
Department of Surgery
University of Nebraska Medical Center
983280 Nebraska Medical Center
Omaha, NE 68198-3280 USA
001-402-559-4581
macarlso@unmc.edu

ABSTRACT

Introduction. Five years survival of pancreatic cancer (PC) remains low. The current murine models may not adequately mimic human PC and can be inadequate for device development. To develop a more accurate large animal model of PC, we induced pancreatic tumors in Oncopigs (transgenic swine expressing *KRAS*^{G12D} and *TP53*^{R167H} mutants).

Methods. Oncopigs (n = 16) were injected via laparotomy with adenovirus expresses Cre recombinase (AdCre) with or without interleukin 8 (IL-8) by either technique 1: into the main pancreatic duct (MPD; via duodenotomy) or by technique 2: into the duct of the isolated pancreatic connecting lobe (CL). Subjects were necropsied after ≤10 week, followed by histological analysis, cytokine expression analysis, exome sequencing and transcriptome analysis.

Results. In a total of 16 OCM subjects, 12 subjects received pancreatic AdCre injection by technique 2 and 9 developed pancreatic tumor (incidence outcome by technique 2: 75%). All of these subjects expired within 2-5 weeks after the tumor induction procedure. All had a similar terminal course: failure to thrive, which was secondary to gastric outlet obstruction, which was secondary to a peripancreatic phlegmon, which was secondary to pancreatitis, which appeared to be secondary to tumor. None of the OCM subjects that underwent a control injection procedure (no AdCre) nor any of the WT littermates that underwent AdCre injection with or without IL-8 developed pancreatitis. Exome and transcriptome analysis of the porcine pancreatic tumors revealed similarity in molecular signatures and pathways with human pancreatic tumors.

Conclusion. Oncopigs developed pancreatic cancer in a short period of time with similar molecular characteristics like human PC. Further optimization to increase the longevity of this

transgenic porcine cancer model will help to investigate the stage-wise progression and therapeutic responses against pancreatic cancer.

INTRODUCTION

Pancreatic cancer (PC) is the 14th most common cancer and the 7th highest cause of cancer mortality in the world.[1] Globally, the number of deaths, incident cases, and disability-adjusted life-years had doubled from 1990 to 2017.[2] Patients with Stage I PC (tumor is less than 2.0 cm with no involved lymph nodes)[3] have a 39% 5-year survival while patients with Stage IV PC (tumor of any size with distant metastases) have an 11% 5-year survival.[4] Surgical resection is the only chance for a cure, but only 15-20% of patients have resectable disease.[3] Despite the development of multimodal therapy, long-term survival is achieved for only 5% of patients.[5]

Due to ethical and practical concerns regarding human experimentation, animal models have become essential in cancer research;[6] murine models in particular have been used in the preclinical study of pancreatic cancer,[7-10] including xenografted immunodeficient models, genetically engineered mouse (GEM) models, humanized mice, and *in vivo* edited mice.[10-19] While murine modeling has produced tremendous advances in the understanding and treatment of cancer in general, the fact remains that only a few percent of drug candidates identified in preclinical studies as potential anti-cancer treatments will be demonstrated to be safe and efficacious in clinical trials, with subsequent FDA approval.[8, 18, 20, 21] Murine models frequently have less-than-ideal accuracy in predicting human biology and response to interventions, secondary to differences in genomic sequence and phenotype; this inaccuracy may contribute to the above inefficiency of the drug pipeline for cancer therapeutics.[10-12, 14, 15]

Currently there are no large animal models for PC. Swine have shown to be effective models in other fields, including trauma, transplantation, cardiovascular disease, and dermatologic conditions.[22, 23] Swine have greater similarity to humans with respect to size, anatomy, physiology, pathophysiological responses, and genetic sequence than do mice.[24, 25] It

therefore is conceivable that swine could have greater accuracy in cancer modeling than mice. Importantly, the human-relevant size of certain porcine breeds allows for research and development of devices, imaging techniques, interventional technologies, and so forth, which would be difficult if not infeasible in an approximately twenty-gram mouse.

Concurrent with the sequencing of the porcine genome and the increased availability and tractability of genetic editing technologies, work has ensued on porcine cancer modeling, including for breast, liver, colorectal, and pancreatic tumors.[26-30] In 2015, a transgenic swine known as the Oncopig Model (OCM) was described,[31] which utilized a Cre-Lox system to control expression of a somatic cassette containing porcine *KRAS*^{G12D} and *TP53*^{R167H}. The expressed KRAS mutant was constitutively activated, while the p53 mutant functioned as a dominant negative. The OCM is the porcine analogue of the KPC mouse.[32] Previously we attempted induction of PC in the OCM with introduction of relatively low doses of adenovirus expressing Cre recombinase (AdCre) into the OCM pancreatic duct, but we did not obtain tumor.[33] Herein we report modification of the AdCre injection protocol to effectively induce PC in the OCM, with resultant tumor generation. This study also characterizes the pancreatic tumors in these pigs by exome and transcriptome analysis and compares with human pancreatic tumors.

MATERIALS AND METHODS

Standards, Rigor, Reproducibility, and Transparency

To the extent possible, the animal studies of this report were designed, performed, and reported in accordance with both the ARRIVE recommendations (Animal Research: Reporting of *In Vivo* Experiments)[34] and the National Institutes of Health Principles and Guidelines for Reporting Preclinical Research;[35] for details and exceptions, refer to Supplemental Information.

Animal Welfare Statement

The animals utilized to generate the data for this report were maintained and treated in accordance with the *Guide for the Care and Use of Laboratory Animals* (8th ed.)[36] and also, in accordance with the Animal Welfare Act of the United States (U.S. Code 7, Sections 2131 – 2159). The animal protocol pertaining to this manuscript was approved by the Institutional Animal Care and Use Committee (IACUC) of the VA Nebraska-Western Iowa Health Care System (ID number 1124) and by the IACUC of the University of Nebraska Medical Center (ID number 19-053-FC). All procedures were performed in animal facilities approved by the Association for Assessment and Accreditation of Laboratory Animal Care International (AAALAC; www.aaalac.org) and by the Office of Laboratory Animal Welfare of the Public Health Service (grants.nih.gov/grants/olaw/olaw.htm). All surgical procedures were performed under isoflurane anesthesia, and all efforts were made to minimize suffering. Euthanasia was performed in accordance with the AVMA Guidelines.[37]

Experimental Subjects

Transgenic Oncopigs (Oncopig Model, or OCM) and their wild type (WT) littermates were purchased from the National Swine Research and Resource Center (NSRRC) at the University of Missouri Columbia (nsrrc.missouri.edu). The OCM subjects were a hybrid of Minnesota minipigs and domestic pigs. Genotype of each porcine subject was confirmed with PCR upon subject delivery (Supplementary Fig. S1). Swine were housed two littermates per pen, except for one week of individual housing post-laparotomy (but still with contact through the pen grating), in order to prevent wound cannibalism. Swine were fed ad lib with standard hog feed (Purina Nature's Match® Sow and Pig Complete Feed; www.purinamills.com).

Reagents

Ad5CMVCre-eGFP (AdCre) was purchased from University of Iowa Vector Core (vector-core.medicine.uiowa.edu). Porcine IL-8 was purchased from Novus Biological (NBP2-35234; novusbio.com). General chemicals were purchased from Millipore Sigma (www.sigmaaldrich.com).

Experimental Design.

The basic experimental design included a ≥1 week acclimatization period after subject delivery to the research facility. PCR confirmation of genotype was performed during this period. Each subject then would undergo an induction procedure (laparotomy under general anesthesia; one major survival procedure), followed by an observation for up to 3 months.

Survival Procedure: Set-Up and Anesthesia

Swine was fasted for 24 hours prior to the procedure, with free access to water. On day zero, subjects were weighted, and underwent induction with ketamine (2.2 mg/kg), Telazol® (1:1 w/w tiletamine:zolazepam, 4.4 mg/kg) and xylazine (2.2 mg/kg), given as a single IM (intra-mascular) injection. EKG, pulse oximetry, and lingual end-tidal CO_2 monitors were placed and connected to a BM5 Bionet monitor (bionetus.com). Endotracheal intubation was performed with a 6-7 mm ID tube. The subject rested on a water-circulated warming blanket that was set at 102˚F. An auricular intravenous (IV) line was placed, and LR was administered at 500mL/hr. Cefovecin sodium (Convenia®; 8 mg/kg IM) and Buprenorphine SR (0.2mg/kg SC) were administered during the induction period. Anesthesia was maintained with isoflurane (1-2%) and supplemental oxygen (3-5 L/min) using Matrx® ventilator (midmark.com). The ventilator rate initially was set at 12-15 breaths per minute with a tidal volume of 8 mL/kg, and subsequently adjusted to maintain the EtCO2 at 40-50 mm Hg. Phlebotomy was performed on a forelimb or auricular vein. The ventral abdomen, groins, and thorax were scrubbed with chlorhexidine soap, and then the ventral abdomen was depilated with electric clippers. Cotton blankets were placed over non-surgical areas to minimize subject heat loss. The final abdominal preparation was performed with alcohol-based chlorhexidine (ChloraPrep™; bd.com), and then the upper midline region was sterilely draped.

Survival Procedure: Tumor Induction

Laparotomy and Exposure. A 12 cm upper midline laparotomy incision was made. Abdominal wall retraction was maintained with a self-retaining abdominal (Bookwalter) retractor. The long tongue of the spleen was placed into the right upper quadrant. The small intestine was held inferiorly with laparotomy pads and the self-retaining retractor. The pylorus

was identified, grasped, and brought up to the incision. The proximal pancreas could be elevated with the pylorus and proximal duodenum; this maneuver provided access to both the anterior and posterior surface of the proximal pancreas (see Results and Discussion). The colon typically was lightly adherent to the anterior surface of the pancreas with loose connective tissue, so the colon was mobilized inferiorly with scissors.

Injection of Tumor Induction Reagent. There were three basic techniques of injecting the tumor induction reagent into the pancreas: (1) injection into the main pancreatic duct with parenchymal injections; (2) injection into the duct of the connecting lobe of the pancreas; and (3) technique 2 plus parenchymal injections. The induction reagent consisted of AdCre (adenovirus expressing Cre recombinase) at a concentration of $1x10^{10}$ PFU/100 µL (in saline), with an injection volume of 200 µL. Some subjects (see Results and Discussion) also received porcine IL-8 (5 ng/mL; 200 µL volume) mixed in with the AdCre, and given as one injection.

Technique 1: Main Duct + Parenchyma. After the above exposure of the pancreas had been obtained, a 3-cm longitudinal enterotomy was made on the anti-mesenteric side of the duodenum, directly opposite to the termination of the duodenal lobe of the pancreas into the duodenal wall, which was the location of the papilla of the main pancreatic duct (MPD). The incised duodenal walls were retracted laterally with silk stay sutures. The MPD then was directly cannulated with a 20-gauge plastic catheter (Angiocath™ IV Catheter; Becton Dickinson) and injected with the induction reagent. Parenchymal injections were also performed in some subjects on the anterior and posterior side of the proximal duodenal lobe of the pancreas (typically two injections on each side, using a 25-gauge needle). Each parenchymal injection site was marked with small dot (1-2 mm

wide) of India ink, using a 27-gauge needle. The duodenal enterotomy then was closed in two layers, using a running 3-0 polyglactin 910 suture for the inner row, full thickness, inverting (Connell) technique. This was followed with an outer seromuscular row of interrupted 3-0 silk sutures (Lembert technique).

Technique 2: Connecting Lobe. After exposure of the pancreas was obtained, the connecting lobe of the pancreas was identified where it joined the proximal duodenal lobe (see Results & Discussion). The connecting lobe then was doubly clamped and transected about 1 cm inferior to the junction with the duodenal lobe. The proximal stump of the connecting lobe (against the duodenal lobe) was tied off with a 3-0 silk ligature. Using operative loupe (3.5x) magnification, the open end of the primary duct running through the connecting lobe was found in the free cut end of that lobe (see Results and Discussion). This duct was cannulated with a 20-gauge plastic catheter, and the induction reagent was injected into the duct of the connecting lobe. The catheter was withdrawn, and the free end of the connecting lobe then was immediately ligated with 3-0 silk.

Laparotomy Closure. The abdominal incision was closed anatomically in layers, with running 3-0 polyglactin 910 in the peritoneum and posterior sheath, running 0-polydioxanone in the anterior aponeurosis, 3-0 polyglactin 910 in the panniculus carnosus, and 4-0 polyglactin 910 in the dermis. Cyanoacrylate glue was applied over the skin incision; no other incisional dressing was applied. The animal's recovery from anesthesia was monitored until the subject was awake and mobile. Subjects were given half feeds on post-induction day 1 and were placed back on ad lib feeds by day 2.

Study Termination and Euthanasia

The prescribed post-induction observation period was three months. Criteria for early removal from the study and euthanasia were symptoms of failure to thrive (anorexia, lethargy, decreased movement, abnormal breathing, or other signs of distress) or sepsis (fever, wound disruption or drainage). At the time of euthanasia, each subject received sedation with ketamine/Telazol/xylazine, as described above, and then endotracheally intubated. Inhalational isoflurane (5%) was administered via the ventilator. The prior midline incision was reopened. Inferiorly this incision was extended in paramedian fashion to avoid midline structures such as the urethra in males. The necropsy incision extended from xiphoid to the pelvic inlet. The bilateral thoracic cavity was entered by transversely incising the diaphragm just inferior to the xiphoid. The intrathoracic portion of the inferior vena cava was easily identified as it emerged from the liver in the posterior mediastinum. Phlebotomy was performed from the cava, and then Fatal-Plus® (pentobarbital sodium, 390 mg/mL; 1 mL per 4.5 kg body weight) was administered by caval injection. Two minutes after administration of Fatal-Plus®, the inferior vena cava was transected just above the diaphragm to exsanguinate the subject. A gross necropsy involving the lungs, heart, liver, kidneys, pancreas, intestines, bladder, and associated peritoneal surfaces then was performed, with biopsy of any suspicious lesions.

Tissue processing, Histology and Immunohistochemistry

Tissue was either formalin fixed and sent for further processing, or fresh tissue was taken and digested for *in vitro* analysis. Tissue that was cut from formalin-fixed samples was stained with H&E for pathological examination. IHC was performed by deparaffinizing slides and heating using citric acid antigen retrieval buffer (Vector laboratories, H3300). Following antigen

retrieval, endogenous peroxidases were quenched with 3% hydrogen peroxide solution for 5 min. Blocking was done using 2.5% goat serum blocking buffer. Primary antibodies used were incubated overnight at 4ºC and are listed in Supplementary Table S1. Vector Laboratories (vectorlabs.com) ImmPress® goat anti-mouse (MP-7452) or anti-rabbit (MP-7451) IgG polymer kits were used for primary antibody detection per the manufacturer's instructions. Detection of the HRP/ peroxidase enzyme was performed with SignalStain® DAB Substrate Kit from Cell Signaling (cat. no. 8059; www.cellsignal.com), per the manufacturer's instructions. Alcian blue staining was performed using the alcian blue stain kit (pH 2.5, Mucin Stain) from abcam (cat. no. ab150662; www.abcam.com). For each group 4 different samples were taken at 20X or 40X magnification and quantification was performed using the automated digital image analysis software ImageJ.

Cytokine Analysis

Blood was extracted via a syringe before surgery and after necropsy. The blood was collected in a 10mL heparin tube to prevent coagulation. Following collection, plasma was extracted per Eve Technologies sample preparation protocol found at evetechnologies.com (detail in Supplemental methods). The samples were then outsourced for analysis. Eve Technologies ran a cytokine/chemokine array 13- plex (PD13) that looked at 13 different markers using the Millipore MILLIPLEX kit. Samples were detected through multiplex immunoassay analyzed with a BioPlex 200. The accuracy/ percent recovery for each cytokine/chemokine analyzed is between 92-103%.

Exome sequencing and analysis

Exome sequences were captured from tumor genomic DNA by SeqCap EZ HyperCap Exome capture probes, designed for pigs (Roslin Pig Exome Design Version 1) according to manufacture protocol (Roche Sequencing and Life Science, Wilmington, MA, USA) and sequenced on NextSeq500 (Illumina Inc., San Diego, CA, USA). The sequences were merged and trimmed by fqtirm tool (https://ccb.jhu.edu/software/fqtrim) to remove adapters, terminal unknown bases (Ns) and low quality 3' regions (Phred score < 30) and processed by bcbio-nextgen 1.2.4 (https://doi.org/10.5281/zenodo.3564938) tool kit with QC (quality control) check by MultiQC 1.9, alignment by bwa, and variant calling by FreeBayes, GATK-HaplotypeCaller, and SAMtools. Variants were called ≥ 2 among the three variant callers to generate the final VCF (variant call format) file. The bcftool in SAMtools was used to generate a single common VCF file for each comparison group and was also used to generate a unique VCF file for each sample in each comparison. The VCF files were then subjected to VEP (variant effect predictor) tool to annotate and predict the effects of each variant. Finally, Circos were used to visualize the variants on pig reference genome.

Transcriptomic analysis

Total RNA was isolated from normal pig pancreas and pancreatic tumor samples using AllPrep DNA/RNA Kits (Qiagen, Germantown, MD, USA), analyzed for RNA integrity score (RIN) by TapeStation System (Agilent, Santa Clara, CA, USA) and hybridized on Porcine Gene 1.1 ST array (Thermo Fisher Scientific, Waltham, MA, USA). The data was quality checked, nornamlized and analyzed on Transcriptome Analysis Console (Agilent, Santa Clara, CA, USA). GESA (Gene Set Enrichment Analysis) was used to identify enriched expression signatures in the tumor samples.

Statistics and Power Analysis

Data are reported as mean ± standard deviation. Statistical analysis was performed using t-test or two-way ANOVA as indicated. $P < 0.05$ was considered to be a statistically significant difference.

RESULTS & DISCUSSION

Cadaveric Anatomical Dissection

The tri-lobar structure of the pancreas has previously been described.[38] In humans, the pancreas has been given somewhat arbitrary anatomical boundaries of "head" (adjacent to the duodenum and to the right of the portomesenteric vein), "neck" (overlying the portomesenteric vein), "body" (to the left of the portomesenteric vein), "tail" (near the splenic hilum), and a variably present uncinate process which comes off the inferior side of the pancreatic head.[39] In the pig, however, there are three fairly distinct lobes which interconnect to form the pancreas: the duodenal, splenic, and connecting lobes (Fig. 1A). The duodenal lobe of the porcine pancreas (Fig. 1A-B) is an elongate structure situated inferiorly to the pylorus and gastric antrum. The proximal end of the duodenal lobe tapers to a termination on the mesenteric border of duodenal C-loop, 10-15 cm distal to the pylorus. At this point the main pancreatic duct traverses the duodenal wall and opens into the duodenal lumen via the pancreatic papilla. The splenic lobe of the porcine pancreas (Fig. 1A-B) is another elongate structure which initiates at the distal end of the duodenal lobe and terminates near the splenic hilum.

The connecting lobe of the porcine pancreas (Fig. 1A-D) is a structure unique to the pig and has no real equivalent in humans. The connecting lobe is a U-shaped structure which connects the mid-portion of the duodenal lobe to the mid-portion of the splenic lobe. This tri-lobar configuration forms a continuous ring of the porcine pancreas, within which runs a continuous circular ductal system (Fig. 1B). This circular configuration is reminiscent of the arterial Circle of Willis at the base of the human brain. The main pancreatic duct of the pig exits from this circular ductal system within the duodenal lobe (Fig. 1B), and continues proximally to enter the duodenum, as described above. This unique circular anatomy of the porcine pancreas

affords a unique surgical opportunity, in that the ring could be safely interrupted for an intervention (e.g., ductal injection, Fig. 1C-D). After such an interruption, the ductal system should be capable of retrograde decompression away from the interruption point, and not be obstructed—if it is assumed that the circular ductal system of the porcine pancreas is indeed a complete circle.

Connecting Lobe Injection in WT Pigs

As mentioned in the introduction, we had previously attempted tumor induction in the OCM (N = 5) but did not obtain gross tumor after 4 months of observation.[33] For those induction procedures, AdCre (the induction reagent) was injected into the main pancreatic duct and parenchyma of the duodenal lobe (Technique 1 in the Methods) at a dose of 1×10^8 pfu. Some histologic abnormalities were noted (proliferative ductal lesions), but none of these appeared to be cancerous. Of note, Schook et al.[40] observed a diffuse nodular thickening of the main pancreatic duct which histologically appeared to be adenocarcinoma in one OCM subject, 12 months after intraductal injection of 4×10^9 pfu of AdCre. We hypothesized that if we increased our dose of AdCre that was injected into the pancreatic duct, then we should obtain ductal cancer in the OCM.

One issue that we noted with our previous group of OCM subjects[33] was that after injection of AdCre into main pancreatic duct, the continual flow of pancreatic secretion rapidly flushed the injectate out of the papilla and into the duodenal lumen. This flushing rapidly diluted the AdCre, likely decreasing its efficacy. In order to prevent this flushing, the pancreatic duct would need to be ligated. However, ligation of the main pancreatic duct would obstruct the entire ductal system (Fig. 1A-B), which presumably would have profound and dangerous consequences

for the subject. We hypothesized that we could instead transect the isthmus region of the proximal connecting lobe (Fig. 1A-D), cannulate and inject a pancreatic duct in this location, and then immediately ligate the duct ends with impunity. This maneuver would minimize loss of the injectate, which thus would be in contact with the ductal epithelium for a longer duration than had the duct not been ligated.

In order to determine whether interruption of the isthmus portion of the connecting lobe with cannulation of the pancreatic duct within the connecting lobe (Fig. 1A-D) would feasible and well-tolerated, we undertook this procedure in WT domestic pigs (N = 5; 3–4 months, 30-45 kg), injecting saline distally into the connecting lobe, with ligation of both cut ends of that lobe (i.e., infection technique 2 in the Methods). This effectively interrupted the circular configuration of the porcine pancreas. At operation, the duct within the transected connecting lobe was small (≤1 mm) but could accommodate insertion of a 20-gauge plastic catheter (Fig. 1B) and flushed easily with 1.0 mL of saline. All five pigs tolerated the connecting lobe injection procedure without difficulty. All pigs underwent necropsy one month after operation, and there was no gross evidence of pancreatic inflammation (data not shown).

Induction of Tumor in OCM Subjects: Technique 1

As discussed above, we elected to give a higher dose of AdCre (2×10^{10} pfu) with the current experiments than what we used before (1×10^{8} pfu), which represented more than a 100-fold increase in the dose of AdCre. We also elected to administer IL-8 as an adjunct with the AdCre; this cytokine has been shown to mobilize the adenoviral receptor to the luminal membrane of epithelial cells, thereby enhancing viral entry.[41, 42] With these two conditions we intended to increase our chances for successful pancreatic tumor induction in the OCM.

The first subject (ID. 468, Table 1) underwent induction with technique 1 (i.e., AdCre + IL-8 injection into the main pancreatic duct + injections into the parenchyma of the duodenal lobe); see Fig. 2A. This subject died unexpectedly over a weekend 17 days after the induction procedure. The carcass was refrigerated, and the necropsy was performed 72 hours later. The subject had gastric perforation with extensive peritoneal soilage (Supplementary Fig. S2A). The cause of the gastric perforation was gastric outlet obstruction, which in turn was caused by a peripancreatic phlegmon (Supplementary Fig. S2B). Unfortunately, reasonably intact tissue could not be obtained for histology secondary to the prolonged interval between death and necropsy. The second subject (ID. 469, Table 1) underwent a similar tumor induction and underwent euthanasia/necropsy on day 73 (planned endpoint), with no gross or microscopic evidence of tumor.

We hypothesized that injecting reagents into the main pancreatic duct was not allowing efficient AdCre action secondary to the flushing phenomenon described above. We therefore elected to perform connecting lobe injection (technique 2 in methods) in all subsequent tumor inductions. We also decided to forgo the concomitant parenchymal injections, secondary to the concern that a parenchymal injection would expose a wide variety of cell types (pancreatic ductal cells, islet cells, fibroblasts, endothelial cells) to AdCre and possible transformation. Pleomorphic or sarcomatous tumor induction with non-directed AdCre injection in the OCM has been observed by Schook's group.[31, 40] We reasoned that injection of AdCre exclusively into a pancreatic duct should keep viral exposure mostly confined to the epithelial cells lining the lumen of the duct, and therefore produce tumor that would be (mostly) an adenocarcinoma.

Induction of Tumor in OCM Subjects: Technique 2

Pancreatic tumor induction with AdCre injection into the connecting lobe (technique 2) was attempted in 12 OCM subjects (Table 1). Only two of these subjects (ID. 473 and 475, Table 1) lived to their planned euthanasia data without incident and had no remarkable findings at gross necropsy nor with microscopic analysis. However, nine of these subjects (75%) had onset of lethargy and decreased feeding at 10-15 days after the induction procedure, with progressive decline that necessitated unplanned euthanasia at a mean of 18 ± 7 days (range 10-31). The gross findings at necropsy in these nine subjects was similar to that in OCM no. 468 above (technique #1; unexpected death), that being a peripancreatic phlegmon producing gastric outlet obstruction (Fig. 2B, Supplementary Fig. S2C). In each case the phlegmonous process had obliterated the region in and around the proximal pancreas; in some cases, there was gross liquefaction. It was difficult to discern anatomical landmarks around the phlegmon. In addition, six of the subjects with tumor had a varying number of intraabdominal nodules (<1 cm) studding the surface of various structures (Supplementary Fig. S2D), including the omentum, mesentery, diaphragm, liver, spleen, parietal peritoneum, stomach, and intestines.

The initial concern was that AdCre injection into the connecting lobe of the OCM subjects was inciting a severe pancreatitis that indirectly lead to subject demise from gastric outlet obstruction. However, upon cutting into the phlegmon of these subjects, there was a firm pale core, which appeared to be tumor (Fig. 2C). H&E microscopy of slices taken from the core of the peripancreatic phlegmon from all nine subjects that underwent premature euthanasia demonstrated wide regions of tumor (Fig. 2D-F). Tumor cells had large nuclei with prominent nucleoli. Tumor cell morphology varied from spindle-shaped to rounded. Sheets of tumor cells were interspersed with normal appearing pancreatic acini and the occasional islet, along with areas of liquefaction necrosis and hemorrhage. Areas of tumor were often surrounded by areas of

activated lymphocytes (Fig. 2D-E). In addition, there were numerous tumor-infiltrating lymphocytes and macrophages, and occasionally neutrophils and eosinophils. In some subjects there were numerous multi-nucleated giant cells which appeared to be engulfing vacuoles of necrotic material.

Immunohistochemistry of tumor samples from the peripancreatic phlegmon stained positive for mutant $Kras^{G12D}$ and mutant p53 (Fig. 3A). Quantification of positively stained mutant $Kras^{G12D}$ and mutant p53 cells were statistically significant and revealed an approximately 70% and 40% increase in tumor samples compared to control samples, respectively (Fig. 3B). Tumors also had an increase in Ki-67 and alcian blue staining (Fig 3C, D). Quantification of Ki-67 and alcian blue showed a 15% and 30% increase in tumors compared to control samples (Fig. 3D). This result indicates that OCM pancreatic tumors are more proliferative and with increased acidic mucins and hyaluronic acid deposition into the extracellular matrix, which are observed in human pancreatic cancer.[43-45] The tumors were of mixed and dedifferentiated phenotype, showing positive staining for CK19, vimentin and CD31 markers (Fig. 3E). Quantification of CK19 staining showed no significant difference in expression between tumor and control samples (data not shown). We had a cytokine array performed with 3 OCM subjects that were positive for tumors. Cytokine analysis showed increased expression of IL-1β, IL-6, IL-8 and IL-10 cytokines at necropsy compared to pre-surgery serum levels (Fig. 4A, B). These inflammatory cytokines have been shown to be elevated in patients with pancreatitis and pancreatic cancer and are involved in the development and progression of pancreatic cancer.[46]

In the subjects that had tumor nodules outside of the phlegmon, these grossly appeared to be “drop” or contact metastases, being only present on the surface of the involved organ or

tissue, and mostly inferior and ventral to the phlegmon. There was no evidence of nodule formation contained within the body of an organ, such as the liver. Histologic evaluation of these extra-pancreatic nodules revealed them to be dedifferentiated tumor with a prominent component of activated lymphocytes, both around and within the tumor (data not shown). In some cases, these tumor implants showed evidence of invasion into the underlying normal tissue, with disruption of the peritoneum and underlying connective tissue capsule covering the normal tissue (data not shown).

The remaining, as yet undescribed subject (ID. 1088, Table 1) in this group of 12 OCM underwent unplanned euthanasia on day 113 secondary to respiratory distress. At necropsy there was gross evidence of acute pneumonia; on histology, the pulmonary alveoli filled with fluid and acute inflammatory cells. There also were several nodules (≤1 cm) on the surface of the anterior stomach, but the pancreas was unremarkable. Histologic evaluation of the gastric nodules demonstrated dedifferentiated tumor, similar to the above extra pancreatic nodules. This subject also had sheets of activated lymphocytes present on H&E sections of the liver, spleen, and lung. Blood work at necropsy showed an elevated WBC, indicating this subject had a hematological malignancy (data not shown).

Control Injections in OCM and WT Pigs

Similarly, injections of tumor-induction agents (AdCre ± IL-8) into the connecting lobe (technique 2) of non-transgenic pigs (N = 6; WT littermates of the OCM subjects; Table 1) were performed in order to determine whether the procedure or the induction agents would induce any pathology in the background breed of the OCM. All WT subjects tolerated the injection without difficulty, and there was no remarkable finding at necropsy. H&E evaluation of the connecting

lobe of the pancreas in these subjects revealed minimal chronic inflammation, but otherwise was unremarkable. Immunohistochemical staining of Ki67 and alcian blue was significantly low in these control samples as compared to the OCM subjects (Fig. 3C, D). Vimentin, CD31 and CK19 expressed in the control samples as like the OCM subjects (Fig. 3E). Cytokine analysis looking at inflammatory markers in the control samples showed decreased expression in 2 of the controls at necropsy but overall, no correlation was observed in the WT control subjects (Fig. 4B). In order to determine whether some condition unique to the transgenic pig (and not necessarily tumor) was producing severe pancreatitis after the connecting lobe procedure, two OCM subjects underwent IL-8 injection only into the connecting lobe (ID. 1101 and 1087, Table 1). These two subjects tolerated the procedure without difficulty and had no remarkable findings at necropsy. Immunohistochemistry of OCM controls showed similar staining to WT controls with positive staining for CK19, vimentin and CD31 (data not shown). The results of the control injections from both WT and OCM subjects suggested that the severe inflammatory response noted in AdCre-treated OCM subjects was secondary to tumor formation.

Variants in porcine pancreatic tumors found in genes associated with human PDAC

Exome analysis of four pancreatic tumors of Oncopigs shows that insertions and deletions are present in exomic regions of all chromosomes in all four tumor tissues from different Oncopigs (Fig. 5A). Functional variations with high prediction to be able to change protein expression were also present in all the tumors and throughout the exome (Fig. 5B). *KRAS,* the important gene altered in human pancreatic cancer, showed two different types of alterations: deletions and alteration at a known SNP position (Table 2). The exome analysis successfully detected the presence of *KRAS* ^{G12D} mutation in the Oncopigs (Table 2). Another

pancreatic cancer associated gene in humans, *TP53* showed two intronic variants in three OCM tumors that are in a known SNP position (Table 2). One mutation in only one pig tumor was found in *SMAD4* (Table 2).

Apart from these three most common genes of human pancreatic cancer, other relevant genes with PDAC were found to be altered by insertions, deletions, and functionally relevant variations (Table 3 and Fig. 5D). Deletions found in three out four pig tumors in *CCND1*, *CASP9* and in all samples for *ARHGEF6* (Table 3). Insertions and deletions were mostly found in *MAPK10* gene, with occasional presence in *EGF* and *RB1* (Fig. 5C-D). Together, these findings suggest that porcine pancreatic tumors showed similar mutational landscape with human PDAC.

Porcine pancreatic tumors express known genes and pathways linked with human PDAC

Transcriptome of pancreatic tumors from the Oncopigs was compared with normal pancreas of wild type animals. Expression of known pancreatic cancer related genes in human PDAC, e.g., KRAS, P53 was found to be over-expressed in porcine pancreatic tumors (Fig. 6A). Genes associated with cancer related epithelial to mesenchymal transition (EMT) pathways, e.g., MMP3, FN1 and Vimentin, were among the top overexpressed genes in these tumors (Fig. 6A). SERPINI2, a tumor suppressor gene, known to downregulated in several cancers including PDAC,[47, 48] were among the lowest expressing genes in the OCM tumors. Similarly, microRNA mir-217, another potential tumor suppressor gene in PDAC,[49] which targets KRAS expression, was found among the lowest expressing genes of porcine pancreatic tumors.

Hierarchical cluster analysis of top 50 upregulated and down-regulated genes in OCM pancreatic tumors identified 4 major biological processes that are altered in the tumors (Fig. 6B). Matrix metalloproteases were activated with upregulation of IL4 and IL13 signaling in the

tumors, while early pancreatic precursors and genes associated with digestion and absorption were down-regulated (Fig. 6B). Involvement of different MMPs and IL4 and IL13 are known to be associated with progression of human PDAC.[50-52] Specifically, expression of KRAS and P53 was also found to be up regulated in the porcine pancreatic tumors (Fig. 6C). EMT is the other signaling pathway, which is significantly over-represented in OCM tumors (Fig. 6D). EMT is widely known to be an associated process in cancer, especially pancreatic cancer.[53, 54] Genes like, MMP1, MMP3, periostin (POSTN), fibronectin (FN1), tissue inhibitor of metalloproteinase 1 (TIMP-1), regulator of G-protein signaling (RGS4), plasminogen activator urokinase receptor (PLAUR) and integrin subunit beta 3 (ITGB3), were the top enriched genes in the EMT pathways in OCM tumors (Fig. 6E).

This proof-of-principle study demonstrated that tumor could be induced in the pancreas of the *KRAS/TP53* Oncopig. However, the time course was fulminant (sometimes <2 weeks), and the subjects succumbed to a secondary complication of the tumor (gastric outlet obstruction), not necessarily the tumor itself. The intense inflammatory reaction associated with the tumor may have been secondary to an acute load of neoantigens that flooded these juvenile-aged subjects with an intact and vigorous immune system. Another possible cause of this reaction may have been a response to adenoviral infection; however, this is unlikely, since none of the WT pigs similarly treated with AdCre developed pancreatitis.

While pancreatic tumor induction is indeed feasible in the Oncopig, the current status of a porcine model of pancreatic cancer is that further development is needed. The time course of tumor development in this study was too rapid for the model to be amenable for research purposes. The clinical course of tumor development might be slowed by decreasing the current dose of AdCre - with the understanding that prior experiments that used lower doses of AdCre

produced no tumor at all. Another option might be to use a different viral vector (e.g., lentivirus), which might result in lower levels of AdCre expression.

The associated T-cell inflammatory response, which appeared to be a major underlying cause of rapid subject demise, might be mitigated with administration of immunosuppression. However, use of immunosuppression would increase the model complexity and might impact model relevance. The fields of tumor immunomodulation and tumor immunoediting currently are under intense study,[19, 55-57] and tumor interactions with the immune system in these OCM subjects could be highly relevant. Secondary to these realities, and the concerns over clinical relevance of tumor xenografting in immunodeficient mice,[9, 58] it was our intent from the outset of these studies to develop a large animal model of pancreatic cancer in immunocompetent subjects.

Another possible issue with tumor induction in the present study was the pleomorphic and sometimes dedifferentiated appearance of the tumor cell populations. It was not clear whether these tumors were mostly epithelial in nature (i.e., resembling pancreatic ductal adenocarcinoma), or something else. Even though the AdCre was injected into the pancreatic duct, it still may have been possible for AdCre infection and transformation of non-epithelial cells. The frequent presence of intraabdominal drop metastases in the OCM subjects suggested that intraperitoneal spillage of the AdCre during the injection procedure may have occurred, with resultant formation of peritoneally-located tumor nodules. So non-specific transformation may still be an issue, even with the highly specific connecting lobe injection procedure described in this report. This non-specificity might be addressed in the future with a new transgenic pig, derived from the OCM, in which expression of the transgenes would be restricted to ductal epithelium using a tissue-specific promoter.

The exomic analysis of the porcine pancreatic tumors suggested that the genes which are most altered in the human pancreatic cancer, e.g., *KRAS*, *TP53* and *SMAD4* were also altered in these tumors. The frequency of *KRAS* gene alteration in OCM pigs are 50% (two deletions in two out of four Oncopigs), *TP53* is 75% (two variations in known SNP positions in three out of four Oncopigs) and *SMAD4* is 25% (one mutation in one out of four Oncopigs, see Table 1 for details). Although the human PDAC showed a higher penetrance in KRAS mutations (mutation frequency: 74%, combined analysis of 11 studies with 1326 patients, Supplementary table 2), a smaller number of OCM subjects could be a major contributing factor for the observed 50% KRAS mutations frequency in porcine pancreatic tumor. Human PDAC mutation frequency in *TP53* and *SMAD4* are at 53% and 23%, respectively (11 studies with 1326 patients, Supplementary table 2), which comparable with *SMAD4* mutation frequency of 25% in porcine tumors. As the *TP53* genomic mutations in OCM tumors are observed in known SNP positions, the comparison with *TP53* mutation frequency in human PDAC is not straightforward and cannot be concluded clearly as whether similar or different from pig tumors. RNA expression of KRAS and P53 and protein expression of mutant KRAS G12D, mutant P53 were up regulated in OCM tumors (Fig. 6C and 3A), which co-relates with expression of these genes in human PDAC. OCM tumors are also significantly more proliferative than control and expresses significantly more acidic mucins the tumor tissue. The transcriptomics analysis also confirmed the over-expression of several mucins, e.g., MMP3, MMP1, in the porcine pancreatic tumors. Moreover, EMT was significantly enriched in these tumors, with a significant high level of IL-1β secretion in the serum. Human PDAC is known to contain fibroinflammatory stroma, with high levels of mucins, interleukins and EMT associated tissue inhibitors of matrix metalloproteinase (TIMPs).[50, 51, 53, 54] In addition, genes associated with IL4 and IL13 signaling were also found to

be up regulated in OCM tumors, which are known to be a major component of tumor microenvironment (TME) and have significant contributions in progression and metastasis of several cancers including PDAC.[52, 59]

Taken together, it can be concluded that AdCre injection into the connecting lobe (method 2) of the transgenic swine model (LSL-*KRAS*^{G12D}-IRES-*TP53*^{R167H}) generated pancreatic cancer at a frequency of 75%. All had a similar terminal course: failure to thrive, which was secondary to gastric outlet obstruction, which was secondary to a peripancreatic phlegmon, which was secondary to pancreatitis, which appeared to be secondary to tumor. None of the WT littermates that underwent AdCre injection with or without IL-8 developed pancreatitis. The pancreatic tumors generated by the AdCre injection in Oncopigs resemble with human PDAC by genetic mutations observed in known oncogenes and tumor suppressors, similar transcriptomic gene expression signatures, oncogenic protein expressions, aberrant mucin secretions, inflammatory cytokine secretions and similar expression of genes associated with the microenvironment of PDAC.

Table 1. Tumor induction method and outcome in OCM and WT control pigs.

Type of study	Technique	ID	Type	Sex	MPD	CL	AdCre	IL-8	CNI	Day	Euthanasia reason	Gross outcome	Microscopic outcome
Oncopig, AdCre induction	1	468	OCM	M	+	–	+	+	-	17	Died prematurely	PP, GOO	Not available
	1	469	OCM	M	+	–	+	+	-	73	Planned endpoint	Unremarkable	Unremarkable
	2	470	OCM	M	–	+	+	+	-	**12**	Illness	PP, GOO	**Pancreatic tumor**
	2	471	OCM	M	–	+	+	+	-	**14**	Illness	PP, GOO	**Pancreatic tumor**
	2	472	OCM	M	–	+	+	+	-	**14**	Illness	PP, GOO	**Pancreatic tumor**
	2	473	OCM	M	–	+	+	-	-	59	Planned endpoint	Unremarkable	Unremarkable
	2	474	OCM	M	–	+	+	+	-	**22**	Illness	PP, GOO	**Pancreatic tumor**
	2	475	OCM	M	–	+	+	+	-	35	Planned endpoint	Unremarkable	Unremarkable
	2	1102	OCM	M	–	+	+	-	-	**31**	Illness	PP, GOO	**Pancreatic tumor**
	2	1088	OCM	M	-	+	+	-	-	113	Illness	Pneumonia	Pneumonia; peritoneal tumor
	2	1090	OCM	M	-	+	+	+	+	**15**	Illness	PP, GOO	**Pancreatic tumor**
	2	1092	OCM	M	-	+	+	-	+	**14**	Illness	PP, GOO	**Pancreatic tumor**
	2	1095	OCM	F	-	+	+	+	+	**10**	Illness	PP, GOO	**Pancreatic tumor**
	2	1096	OCM	F	-	+	+	-	+	**27**	Died prematurely	PP, GOO	**Pancreatic tumor**
Oncopig, no induction	2	1101	OCM	M	-	+	-	+	-	121	Planned endpoint	Unremarkable	Unremarkable
	2	1087	OCM	F	-	+	-	+	-	121	Planned endpoint	Unremarkable	Unremarkable
Wild type, AdCre induction	2	477	WT	M	–	+	+	–	-	35	Planned endpoint	Unremarkable	Unremarkable
	2	479	WT	M	–	+	+	–	-	36	Planned endpoint	Unremarkable	Unremarkable
	2	481	WT	M	–	+	+	+	-	28	Planned endpoint	Unremarkable	Unremarkable
	2	482	WT	M	–	+	+	+	-	28	Planned endpoint	Unremarkable	Unremarkable
Wild type, no induction	2	476	WT	M	–	+	-	–	-	35	Planned endpoint	Unremarkable	Unremarkable
	2	478	WT	M	–	+	-	–	-	33	Planned endpoint	Unremarkable	Unremarkable

IL-8 = interleukin 8; AdCre = adenovirus expressing Cre recombinase; CL = pancreatic connecting lobe injection (technique #2); CNI = cyclosporine, Day = length of survival after induction, in days; GOO = gastric outlet obstruction; MPD = main pancreatic duct injection (technique #1); OCM = Oncopig model; PP = peripancreatic phlegmon; WT = wild type.

Table 2. New and existing variations in major pancreatic cancer genes of OCM tumors

Genes	Variations	Location	Type	Samples
KRAS	Deletion (GAT) with rs705858787	5:48548834-48548836	3 prime UTR variant, cDNA (4665-4667)	1095, 1096 vs OCM control and Control
	Deletion of rs701486753 (A)	5:48549683	Downstream gene variant	1095, 1096 vs OCM control and Control
	rs329769372 (G/A)	5:48504818	Upstream gene variant	1095 vs OCM control and Control
	Mutation (G/A)	5:48513419	Missense variant (G to D)	1090, 1092, 1095 & 1096 vs Control
TP53	rs336094858 (T/C)	12:52940975	Intron variant (T to C)	1092, 1095 and 1096 vs OCM control
	rs343411452 (T/C)	12:52942629	Intron variant (T to C)	1092, 1095 and 1096 vs OCM control
	rs81211696 (T/G)	12:52941073	Synonymous variant (T to G)	1090, 1092, 1095 & 1096 vs Control
	rs318253531(C/A)	12:52942206	Synonymous variant (C to A)	1090, 1092, 1095 & 1096 vs Control
	rs81211695 (C/T)	12:52942221	Synonymous variant (C to T)	1090, 1092, 1095 & 1096 vs Control
	rs334394956 (G/A)	12:52942644	Synonymous variant (G to A)	1090, 1092, 1095 & 1096 vs Control
	rs324980623 (G/A)	12:52942707	Synonymous variant (G to A)	1090, 1092, 1095 & 1096 vs Control
	rs345021946 (C/A)	12:52942996	Synonymous variant (C to A)	1090, 1092, 1095 & 1096 vs Control
	Mutation (T/C)	12:52943005	Intron variant (T to C)	1090, 1092, 1095 & 1096 vs Control
	Mutation (C/T)	12:52943212	Intron variant (C to T)	1090, 1092, 1095 & 1096 vs Control
SMAD4	Mutation (A/T)	1:100590467	Intron variant (A to T)	1090 vs OCM control and Control

Table 3. Variations and genetic aberrations in pancreatic cancer related genes in OCM tumors

Genes	Number of variations	Type of variations	Samples
AKT1	15	SNPs (15), rsID (0)	All samples
AKT2	12	SNPs (8), rsID (2) | single base splice insertion (2)	All samples (SNPs)
			All vs OCM Control (insertion)
AKT3	30	SNPs (24), rsID (24) | insertions (5), 3 UTR (2), intronic (3) | six base deletion, intronic, with SNPs (1)	All samples (SNPs)
			Insertions in 1090, 92 & 96 vs Control and OCM controls
ARAF	3	SNPs (3), rsID (3)	All vs controls, 1095, 1096 vs OCM controls
ARHGEF6	63	SNPs (59), rsID (59) | one 17bp insertions, intronic (1) | 3 deletions, downstream (2), intron (1)	All samples (SNPs)
			Insertion (1096 vs control, OCM control)
			Deletion (all samples)
BAD	18	SNPs (18), rsID (17)	All samples
BCL2L1	3	SNPs (3), rsID (3)	1095 vs control, all vs OCM Control
BRAF	34	SNPs (34), rsID (34)	All samples
CASP9	106	SNPs (100), rsID (1)	All samples
		13 bp intronic insertions (1)	Insertions in 1096 vs Control and OCM control
		Deletions (4): intronic (3), 3 UTR (1)	Deletions in 1095, 1096 and 1090
CCND1	5	SNP (4), rsID (2) | Insertion single base intronic (1)	All samples
			Deletion: 1090, 92, 96
CDK4	23	SNP (23), rsID (21) | 9 bp insertion intronic (1)	All samples
			1095, 1096 vs Control, OCM control
CDK6	17	SNP (17), rsID (11) | single bp deletion (2), double bp deletion (1), 4 bp deletion (1)	All samples
			1090, 1095 vs Control and OCM control
ERBB2	15	SNPs (13), rsID (13), 5 downstream, 6 intronic, 1 missense, 2 synonymous, 1 upstream | insertion (2)	All samples
RAD51	26	SNPs (26), rsID (25), 11 3 UTR, 10 introns, 1 missense, 1 synonymous, 3 downstream	All samples

References**:**

1. McGuigan, A. *et al.* Pancreatic cancer: A review of clinical diagnosis, epidemiology, treatment and outcomes. *World J Gastroenterol* **24**, 4846-4861 (2018).
2. G. B. D. Pancreatic Cancer Collaborators The global, regional, and national burden of pancreatic cancer and its attributable risk factors in 195 countries and territories, 1990-2017: a systematic analysis for the Global Burden of Disease Study 2017. *Lancet Gastroenterol Hepatol* **4**, 934-947 (2019).
3. National Comprehensive Cancer Network in NCCN Clinical Practice Guidelines In Oncology (NCCN Guidelines®). (ed. NCCN) (NCCN, 26 November 2019).
4. Kamarajah, S.K., Burns, W.R., Frankel, T.L., Cho, C.S. & Nathan, H. Validation of the American Joint Commission on Cancer (AJCC) 8th Edition Staging System for Patients with Pancreatic Adenocarcinoma: A Surveillance, Epidemiology and End Results (SEER) Analysis. *Ann Surg Oncol* **24**, 2023-2030 (2017).
5. van Roessel, S. *et al.* International Validation of the Eighth Edition of the American Joint Committee on Cancer (AJCC) TNM Staging System in Patients With Resected Pancreatic Cancer. *JAMA Surg* **153**, e183617 (2018).
6. Gengenbacher, N., Singhal, M. & Augustin, H.G. Preclinical mouse solid tumour models: status quo, challenges and perspectives. *Nat Rev Cancer* **17**, 751-765 (2017).
7. Olive, K.P. & Tuveson, D.A. The use of targeted mouse models for preclinical testing of novel cancer therapeutics. *Clin Cancer Res* **12**, 5277-5287 (2006).
8. Sharpless, N.E. & Depinho, R.A. The mighty mouse: genetically engineered mouse models in cancer drug development. *Nat Rev Drug Discov* **5**, 741-754 (2006).
9. Siolas, D. & Hannon, G.J. Patient-derived tumor xenografts: transforming clinical samples into mouse models. *Cancer Res* **73**, 5315-5319 (2013).
10. Talmadge, J.E., Singh, R.K., Fidler, I.J. & Raz, A. Murine models to evaluate novel and conventional therapeutic strategies for cancer. *Am J Pathol* **170**, 793-804 (2007).
11. Begley, C.G. & Ellis, L.M. Drug development: Raise standards for preclinical cancer research. *Nature* **483**, 531-533 (2012).
12. Cook, N., Jodrell, D.I. & Tuveson, D.A. Predictive in vivo animal models and translation to clinical trials. *Drug Discov Today* **17**, 253-260 (2012).
13. Day, C.P., Merlino, G. & Van Dyke, T. Preclinical mouse cancer models: a maze of opportunities and challenges. *Cell* **163**, 39-53 (2015).
14. Ebos, J.M. & Kerbel, R.S. Antiangiogenic therapy: impact on invasion, disease progression, and metastasis. *Nat Rev Clin Oncol* **8**, 210-221 (2011).
15. Francia, G., Cruz-Munoz, W., Man, S., Xu, P. & Kerbel, R.S. Mouse models of advanced spontaneous metastasis for experimental therapeutics. *Nat Rev Cancer* **11**, 135-141 (2011).
16. Maddalo, D. *et al.* In vivo engineering of oncogenic chromosomal rearrangements with the CRISPR/Cas9 system. *Nature* **516**, 423-427 (2014).
17. Sanchez-Rivera, F.J. *et al.* Rapid modelling of cooperating genetic events in cancer through somatic genome editing. *Nature* **516**, 428-431 (2014).
18. Singh, M., Murriel, C.L. & Johnson, L. Genetically engineered mouse models: closing the gap between preclinical data and trial outcomes. *Cancer Res* **72**, 2695-2700 (2012).
19. Zitvogel, L., Pitt, J.M., Daillere, R., Smyth, M.J. & Kroemer, G. Mouse models in oncoimmunology. *Nat Rev Cancer* **16**, 759-773 (2016).

20. Kola, I. & Landis, J. Can the pharmaceutical industry reduce attrition rates? *Nat Rev Drug Discov* **3**, 711-715 (2004).
21. Reichert, J.M. & Wenger, J.B. Development trends for new cancer therapeutics and vaccines. *Drug Discov Today* **13**, 30-37 (2008).
22. Swindle, M.M., Makin, A., Herron, A.J., Clubb, F.J., Jr. & Frazier, K.S. Swine as models in biomedical research and toxicology testing. *Vet Pathol* **49**, 344-356 (2012).
23. Swindle, M.M. & Smith, A.C. *Swine in the Laboratory: Surgery, Anesthesia, Imaging, and Experimental Techniques*, Edn. 3rd. (CRC Press, Boca Raton, FL; 2016).
24. Kuzmuk, K.N. & Schook, L.B. Pigs as a Model for Biomedical Sciences, in *The Genetics of the Pig*. (eds. M.F. Rothschild & A. Ruvinsky) 426-444 (CABI, Oxfordshire, UK; 2011).
25. Schook, L.B. *et al.* Unraveling the swine genome: implications for human health. *Annu Rev Anim Biosci* **3**, 219-244 (2015).
26. Bailey, K.L. & Carlson, M.A. Porcine Models of Pancreatic Cancer. *Front Oncol* **9**, 144 (2019).
27. Luo, Y. *et al.* High efficiency of BRCA1 knockout using rAAV-mediated gene targeting: developing a pig model for breast cancer. *Transgenic Res* **20**, 975-988 (2011).
28. Schachtschneider, K.M. *et al.* The Oncopig Cancer Model: An Innovative Large Animal Translational Oncology Platform. *Front Oncol* **7**, 190 (2017).
29. Flisikowska, T., Kind, A. & Schnieke, A. The new pig on the block: modelling cancer in pigs. *Transgenic Res* **22**, 673-680 (2013).
30. Flisikowska, T., Kind, A. & Schnieke, A. Pigs as models of human cancers. *Theriogenology* **86**, 433-437 (2016).
31. Schook, L.B. *et al.* A Genetic Porcine Model of Cancer. *PLoS One* **10**, e0128864 (2015).
32. Hingorani, S.R. *et al.* Trp53R172H and KrasG12D cooperate to promote chromosomal instability and widely metastatic pancreatic ductal adenocarcinoma in mice. *Cancer Cell* **7**, 469-483 (2005).
33. Remmers, N. *et al.* Generation of tumorigenic porcine pancreatic ductal epithelial cells: toward a large animal model of pancreatic cancer. *bioRxiv* **published online 16 February 2018; revised submission 17 May 2018** (2018).
34. Kilkenny, C., Browne, W.J., Cuthill, I.C., Emerson, M. & Altman, D.G. Improving bioscience research reporting: the ARRIVE guidelines for reporting animal research. *PLoS Biol* **8**, e1000412 (2010).
35. National Institutes of Health (
36. Committee for the Update of the Guide for the Care and Use of Laboratory Animals *Guide for the Care and Use of Laboratory Animals.* . (The National Academies Press, Washington, DC; 2011).
37. American Veterinary Medical Association Panel on Euthanasia *AVMA Guidelines for the Euthanasia of Animals: 2020 Edition*, Vol. Version 2020.0.1. (American Veterinary Medical Association, Schaumberg, IL; 2020).
38. Ferrer, J. *et al.* Pig pancreas anatomy: implications for pancreas procurement, preservation, and islet isolation. *Transplantation* **86**, 1503-1510 (2008).
39. Skandalakis, L.J., Rowe, J.S., Jr., Gray, S.W. & Skandalakis, J.E. Surgical embryology and anatomy of the pancreas. *Surg Clin North Am* **73**, 661-697 (1993).
40. Principe, D.R. *et al.* KRAS(G12D) and TP53(R167H) Cooperate to Induce Pancreatic Ductal Adenocarcinoma in Sus scrofa Pigs. *Sci Rep* **8**, 12548 (2018).

41. Lutschg, V., Boucke, K., Hemmi, S. & Greber, U.F. Chemotactic antiviral cytokines promote infectious apical entry of human adenovirus into polarized epithelial cells. *Nat Commun* **2**, 391 (2011).
42. Kotha, P.L. *et al.* Adenovirus entry from the apical surface of polarized epithelia is facilitated by the host innate immune response. *PLoS Pathog* **11**, e1004696 (2015).
43. Kaur, S., Kumar, S., Momi, N., Sasson, A.R. & Batra, S.K. Mucins in pancreatic cancer and its microenvironment. *Nat Rev Gastroenterol Hepatol* **10**, 607-620 (2013).
44. Ogawa, Y. *et al.* Three Distinct Stroma Types in Human Pancreatic Cancer Identified by Image Analysis of Fibroblast Subpopulations and Collagen. *Clin Cancer Res* **27**, 107-119 (2021).
45. Pergolini, I. *et al.* Prognostic impact of Ki-67 proliferative index in resectable pancreatic ductal adenocarcinoma. *BJS Open* **3**, 646-655 (2019).
46. Roshani, R., McCarthy, F. & Hagemann, T. Inflammatory cytokines in human pancreatic cancer. *Cancer Lett* **345**, 157-163 (2014).
47. Wehr, A.Y., Furth, E.E., Sangar, V., Blair, I.A. & Yu, K.H. Analysis of the human pancreatic stellate cell secreted proteome. *Pancreas* **40**, 557-566 (2011).
48. Bergeron, S. *et al.* The serine protease inhibitor serpinE2 is a novel target of ERK signaling involved in human colorectal tumorigenesis. *Mol Cancer* **9**, 271 (2010).
49. Zhao, W.G. *et al.* The miR-217 microRNA functions as a potential tumor suppressor in pancreatic ductal adenocarcinoma by targeting KRAS. *Carcinogenesis* **31**, 1726-1733 (2010).
50. Slapak, E.J., Duitman, J., Tekin, C., Bijlsma, M.F. & Spek, C.A. Matrix Metalloproteases in Pancreatic Ductal Adenocarcinoma: Key Drivers of Disease Progression? *Biology (Basel)* **9** (2020).
51. Tjomsland, V. *et al.* Profile of MMP and TIMP Expression in Human Pancreatic Stellate Cells: Regulation by IL-1alpha and TGFbeta and Implications for Migration of Pancreatic Cancer Cells. *Neoplasia* **18**, 447-456 (2016).
52. Shi, J., Song, X., Traub, B., Luxenhofer, M. & Kornmann, M. Involvement of IL-4, IL-13 and Their Receptors in Pancreatic Cancer. *Int J Mol Sci* **22** (2021).
53. Wang, S., Huang, S. & Sun, Y.L. Epithelial-Mesenchymal Transition in Pancreatic Cancer: A Review. *Biomed Res Int* **2017**, 2646148 (2017).
54. Aiello, N.M. *et al.* EMT Subtype Influences Epithelial Plasticity and Mode of Cell Migration. *Dev Cell* **45**, 681-695 e684 (2018).
55. Wagner, M. & Koyasu, S. Cancer Immunoediting by Innate Lymphoid Cells. *Trends Immunol* **40**, 415-430 (2019).
56. Schumacher, T.N. & Schreiber, R.D. Neoantigens in cancer immunotherapy. *Science* **348**, 69-74 (2015).
57. Vesely, M.D., Kershaw, M.H., Schreiber, R.D. & Smyth, M.J. Natural innate and adaptive immunity to cancer. *Annual review of immunology* **29**, 235-271 (2011).
58. Tentler, J.J. *et al.* Patient-derived tumour xenografts as models for oncology drug development. *Nat Rev Clin Oncol* **9**, 338-350 (2012).
59. Hallett, M.A., Venmar, K.T. & Fingleton, B. Cytokine stimulation of epithelial cancer cells: the similar and divergent functions of IL-4 and IL-13. *Cancer Res* **72**, 6338-6343 (2012).

Fig. 1

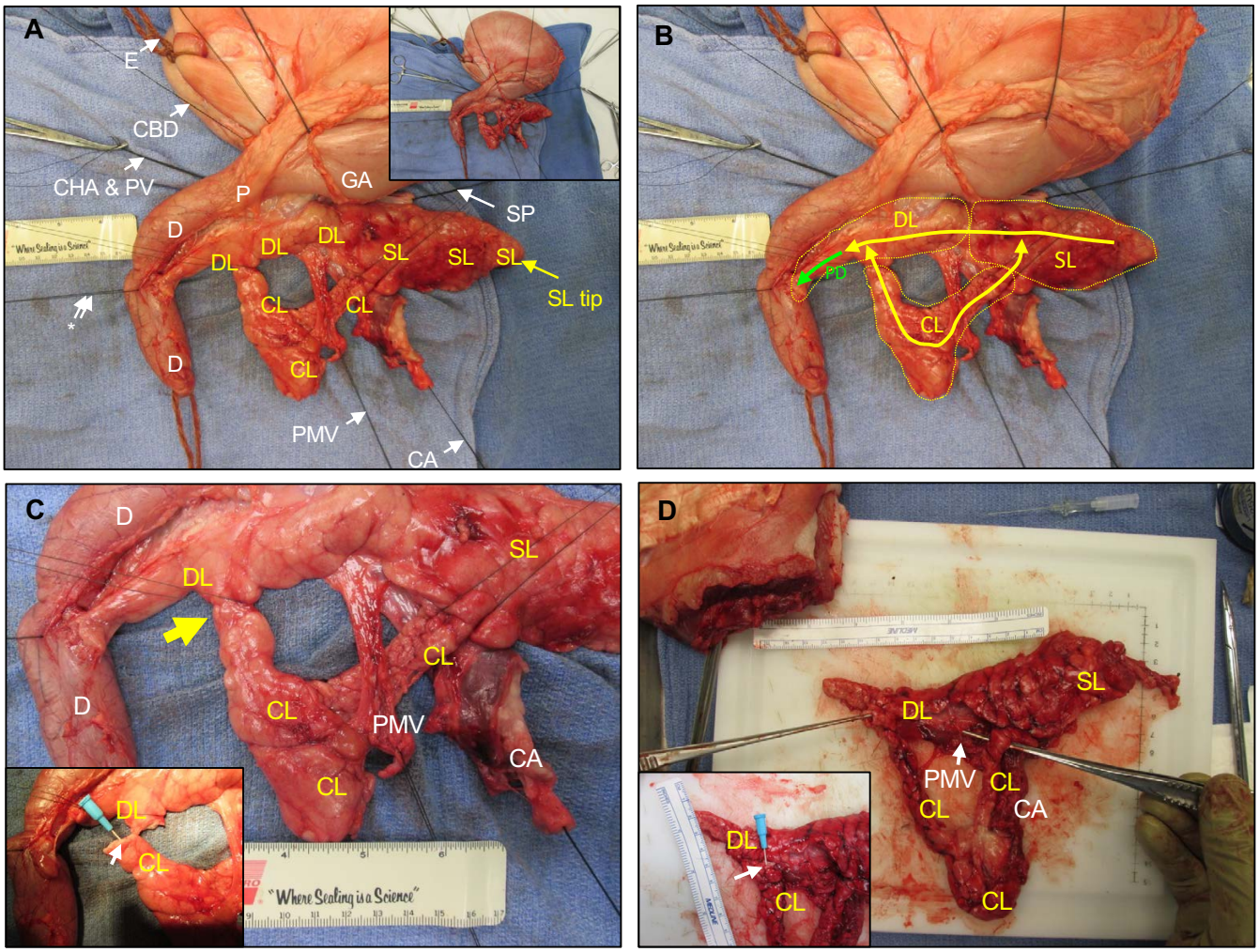

Fig. 1. Porcine pancreatic anatomy. (A) Anterior view, cephalad is at top. Pancreatic lobar architecture: DL = duodenal lobe; CL = connecting lobe; SL = splenic lobe. *Silk stay with double arrow marks approximate site of entry of main pancreatic duct entry into duodenum via the pancreatic papilla (not visible), CA = celiac artery; CBD = common bile duct; CHA & PV = common hepatic artery and portal vein (not visible); E = esophagus; GA = gastric antrum; P = pylorus; PMV = portomesenteric vein emerging from underneath pancreas; SP = splenic pedicle. Inset: zoom out view. (B) Same specimen as panel A. Pancreatic lobar architecture delineated with dashed yellow boundaries. Thick yellow arrows demonstrate approximate course of porcine pancreatic ductal system. The intersections of the DL, SL, and CL form a continuous ductal loop. Interruption of the duct at any given point along this loop would result in pancreatic decompression through the remainder of the loop, from there into the main pancreatic duct (PD, green arrow), out the pancreatic papilla, and into the duodenum. (C) Zoom in view of same specimen. Yellow arrow indicates location of CL transection for injection into the CL duct. Inset: CL has been disconnected from DL; a 22g plastic catheter has been inserted (small white arrow) into the main duct of the CL (mimic of in vivo CL injection procedure). (D) This subject is shown simply for corroboration of panels A-C. But this dissection also demonstrates the full-circle anatomy of the CL, which is connected proximally to the DL and distally to the SL. Inset: cannulization of the CL duct with a 22g plastic catheter; the CL has been transected near its terminus into the DL, similar to that shown in panel C.

Fig. 2

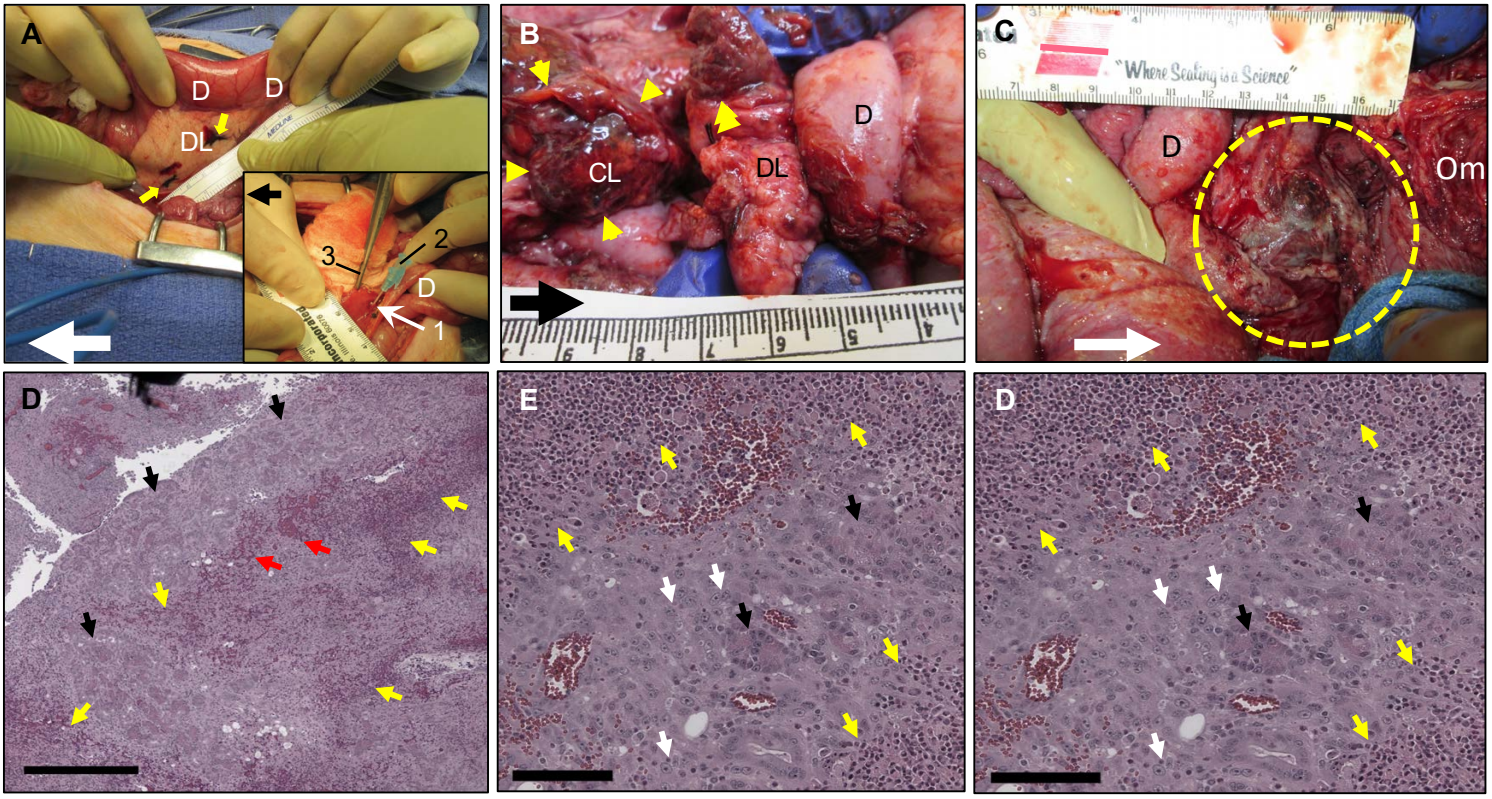

Fig. 2. Induction of pancreatic tumor in Oncopigs. (A) Tumor induction procedure. The pancreas was exposed through an upper midline incision. The posterior surface of the duodenal lobe (DL) of the pancreas was marked at two sites with India Ink (yellow arrows). AdCre was injected into the pancreatic parenchyma. The anterior surface was then exposed, and similar injections were performed into the parenchyma on the anterior pancreas. Next, the duodenal insertion of the main pancreatic duct was identified at the terminus of the duodenal lobe on the mesenteric border of the duodenum. A longitudinal duodenotomy was made on the anti-mesenteric side of the duodenum, just opposite to the insertion of the main pancreatic duct (Inset). The pancreatic papilla (1) was identified within the duodenal lumen and cannulated with a 20g Angiocath (2). Debakey forceps (3) is shown retracting duodenal wall at site of duodenotomy. AdCre was then injected directly into the main pancreatic duct via the papilla. The Angio cath was withdrawn, and the duodenotomy was then closed in two layers. D = duodenum; large white arrow & small black arrow (inset) = cephalad. (B) and (C) Necropsy pictures. (B) The duodenal lobe (DL) was identified, with a silk suture (double yellow arrow) marking the site where the proximal side of the connecting lobe (CL) had been ligated. The remnant of the CL (marked with single yellow arrows) was adjacent to this suture. (C) Dashed line = large phlegmon; D = duodenum; Om = omentum. (D) H&E of involved pancreas. Cords of inflammatory cells (yellow arrows) are intermingled with areas of hemorrhage (red arrows), which surrounded regions of residual acini (black arrows). Bar = 500 μm. (E) Higher power view of phlegmon. Nests of tumor cells are apparent (white arrows), intermingled with residual acinar structures. Bar = 100 μm. (F) High power view; individual tumor cells indicated with white arrows. Bar = 20 μm.

Fig. 3

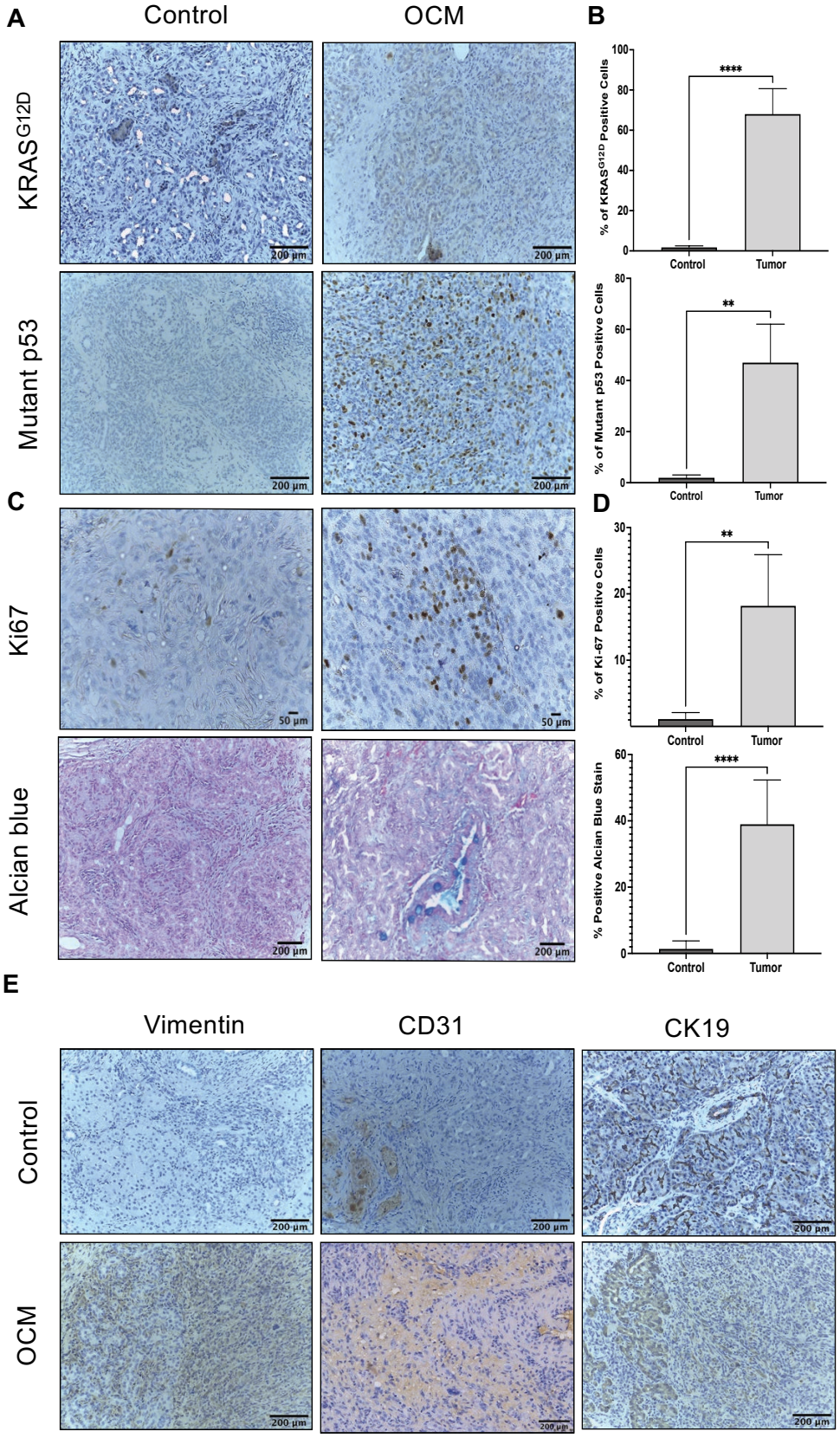

Fig. 3. Pancreatic tumors of the Oncopigs express tumor associated proteins. (A) Expression and (B) quantification of mutant KRAS G12D, mutant p53 showed elevated expression in OCM pancreatic tumors. Staining (C) and quantification (D) of Ki67 and alcian blue also found to be increased in OCM tumors. (E) Vimentin, CD31, and CK19 found to be expressed in OCM pancreatic tumors. The data are presented as the mean ± SD. **P <0.01, ****P <0.0001.

Fig. 4

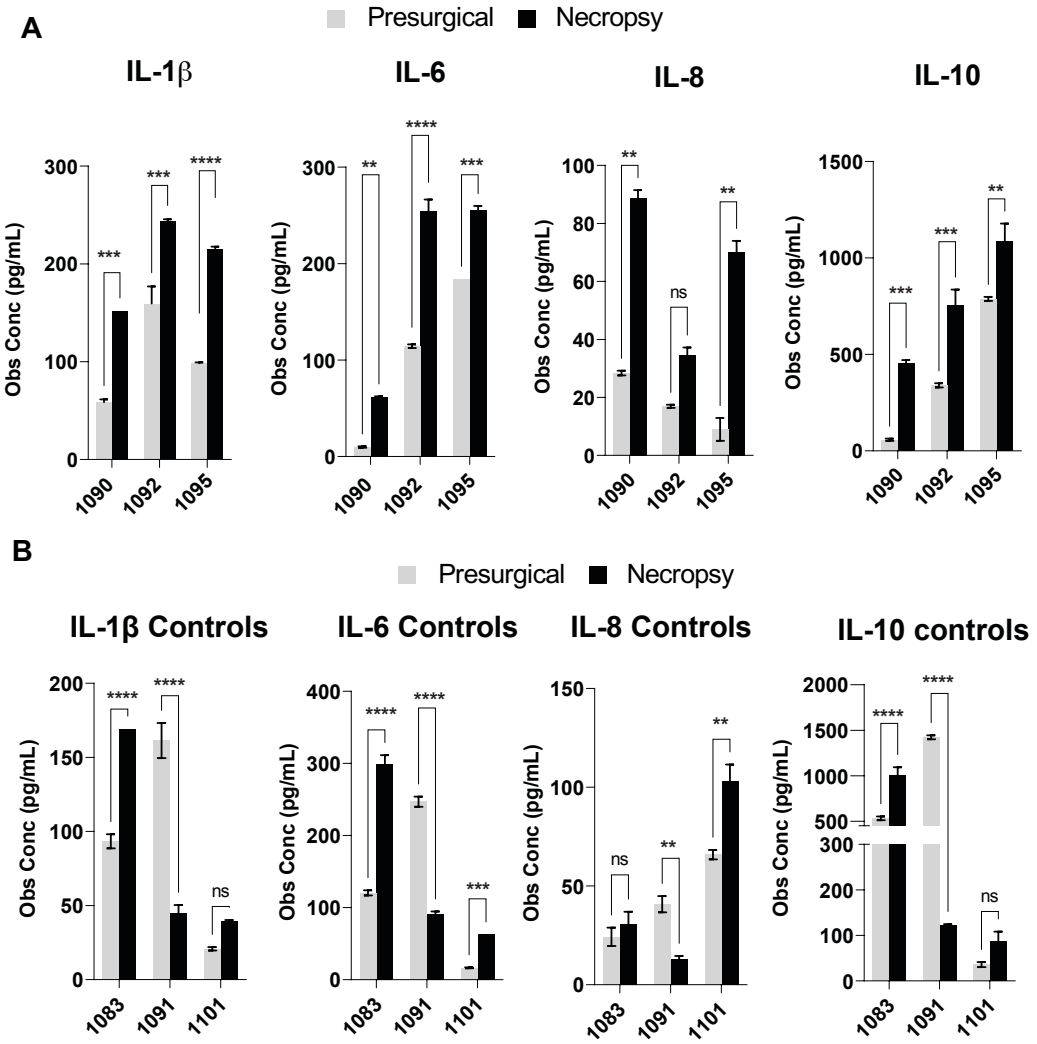

Fig. 4. Cytokine Analysis comparing pre-surgery and necropsy serum levels for tumor and control samples. A-D are all OCM tumor samples. (A) Analysis of IL-1β in 1090, 1092 and 1095. (B) Analysis of IL-6 in 1090, 1092 and 1095. (C) Analysis of IL-8 in 1090, 1092 and 1095. (D) Analysis of IL-10 in 1090, 1092 and 1095. E-H are all control samples. (E) Analysis of IL-1β in 1083, 1091 and 1101. (F) Analysis of IL-6 in 1083, 1091 and 1101. (G) Analysis of IL-8 in 1083, 1091 and 1101. (H) Analysis of IL-10 in 1083, 1091 and 1101. The data are presented as the mean ± SD. ns= not significant, **P <0.01, ***P <0.001, ****P <0.0001.

Fig. 6

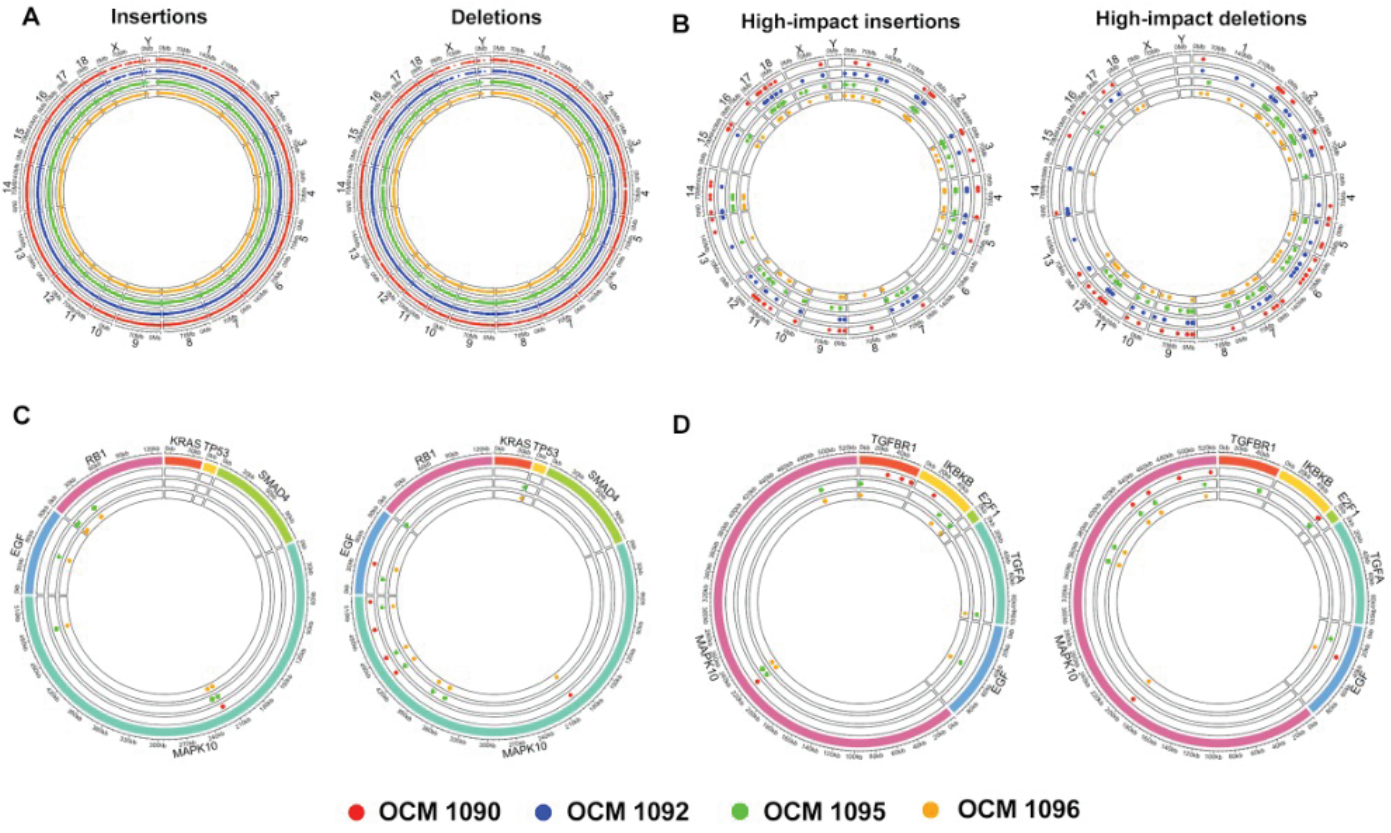

Figure 6: Insertions and deletions in OCM tumors. Exome-wide map of (A) all insertions and deletions and (B) predicted high-impact expression changing insertions and deletions in OCM tumors as compared with exome sequence of OCM pigs without AdCre injection. (C) Insertions and deletions in OCM tumors in (C) known key pancreatic cancer genes and (D) other genes related to pancreatic cancer.

Fig. 6

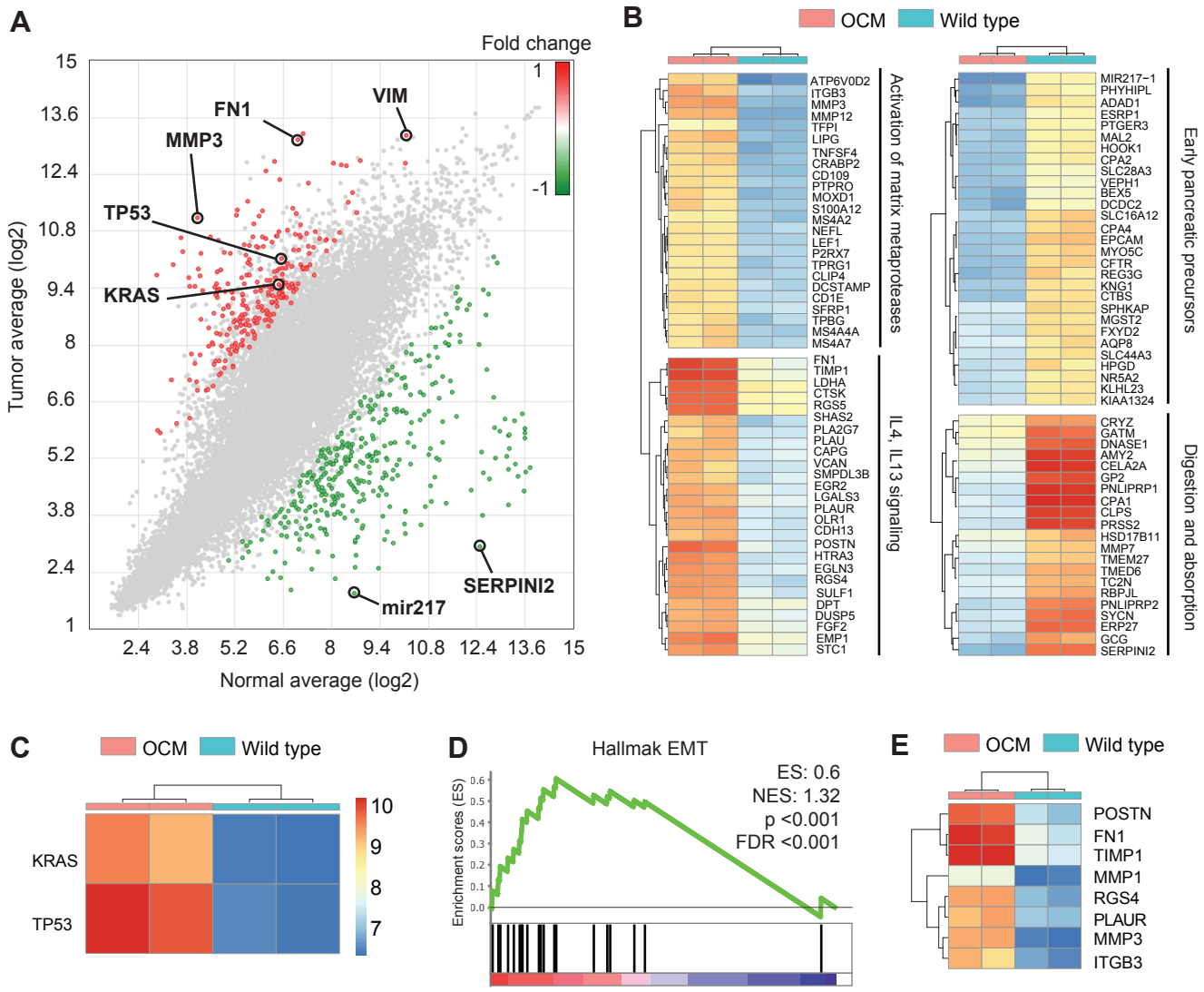

Figure 6. Transcriptome of Oncopig pancreatic tumors vs. normal pancreas. (A) Differential gene expression scatterplot of normal porcine pancreas *vs*. Oncopig pancreatic tumor (RNA-seq data). (B) Hierarchical cluster analysis of top 50 upregulated and down-regulated genes in normal porcine pancreas *vs*. Oncopig pancreatic tumor. (C) KRAS and p53 expression in normal porcine pancreas *vs*. Oncopig pancreatic tumor. (D) Expression score for Hallmark genes of epithelial-mesenchymal transition (EMT) in Oncopig pancreatic tumor. (E) Differential expression of select EMT genes in normal porcine pancreas *vs*. Oncopig pancreatic tumor.